AUT Journal of Modeling and Simulation

AUT J. Model. Simul., 56(2) (2024) 199-208
DOI: 10.22060/miscj.2025.23614.5391

Online Error Estimation of Inertial Measurement Unit in Transfer Alignment Problem

Reza Soltani Nejad, Hamed Mohammad Karimi*, Abolghasem Naghash

Department of Aerospace Engineering, Amirkabir University of Technology, Tehran, Iran.

ABSTRACT: The presence of bias in low-cost inertial sensors has always been a fundamental problem in the estimation of Euler angles. The transfer alignment technique involves using two sets of sensors: a set of low-cost sensors (which may have significant bias) and a set of high-accuracy sensors (which provide reliable data). By comparing the outputs of these two sets, the biases in the low-cost sensors can be estimated and corrected. To achieve this goal, it is necessary to obtain the difference between the master and slave frames. The "master frame" typically refers to the coordinate system defined by the high-accuracy sensors, while the "slave frame" refers to the coordinate system defined by the low-cost sensors. In this article, the method of small rotation angles is used to calculate this difference between the two frames. This article proposes a new alignment algorithm that is both fast and accurate. The biases of accelerometers and gyroscopes can be rapidly estimated and compensated for. The alignment discussed in this article is conducted during motion, which is more complex than stationary mode estimation. The desired maneuver in this study is a constant acceleration maneuver, where the biases of both the accelerometer and gyroscope are well estimated. For other maneuvers, gyroscope biases may not be accurately estimated, while accelerometer biases are generally well estimated. The estimated biases for accelerometers and gyroscopes are often noisy due to errors in the inertial sensors; therefore, preprocessing filtering is also performed to estimate the biases smoothly.

Review History:

Received: Oct. 21, 2024
Revised: Jan. 13, 2025
Accepted: Jan. 14, 2025
Available Online: Jan. 15, 2025

Keywords:

Inertial Navigation System
In-motion Alignment
Transfer Alignment
Bias Compensation
Small Rotation Angles

1- Introduction

Flying vehicles typically begin navigation by performing an 'initial alignment' [1], which involves correcting their directions at the start of a flight. Alignment refers to the relationship between the Body (B) and Navigation (N) coordinate systems [2]. 'Leveling' involves calculating the angles of roll and pitch, representing the vehicle's deviation from the horizon. 'Gyrocompassing' is the process of determining the direction of geographic north.

Inertial alignment is divided into two categories: "stationary alignment" [3, 4] and "in-motion alignment" [5&6]. Stationary alignment is completed in two consecutive steps, improving accuracy in each step. These stages are "coarse alignment" [7 & 8] and "fine alignment" [9 & 10]. The first step (coarse alignment) provides a rough estimate of initial attitudes [11]. In the second phase (fine alignment), a filter is used to correct the alignment and estimate the inertial sensor errors before flight [12].

Coarse alignment offers good estimation speed but lacks accuracy, while fine alignment has lower speed but higher accuracy. Recent research has focused on enhancing the accuracy of coarse alignment and the speed of fine alignment [5, 13]. In [4], by improving the convergence speed of filters, estimation speed in accurate alignment can be enhanced up to 40%.

Transfer alignment is a method used to estimate attitude differences between two inertial platforms with slight mismatches known as misalignment. Challenges in estimating misalignment include validity in small rotation angles and difficulty in estimation with structural deformations. Recent research has addressed these issues [14] and [15-17].

This article focuses on estimating gyroscope and accelerometer biases using a novel method called "differential alignment", combining the speed of coarse alignment with the accuracy of fine alignment. In this algorithm, the rate of change of the small rotation angles is utilized to estimate the misalignment.

The article is organized as follows: Section 2 discusses rewriting navigation error equations, calculating accelerometer and gyroscope bias using master and slave data, and presenting the mathematical formulation of the new algorithm. Section 3 covers the simulations, section 4 presents and analyzes the results, and section 5 concludes the article.

*Corresponding author's email: h.mohammadkarimi@aut.ac.ir

2- Algorithm Formulation

In this section, the equations that obtain the bias of accelerometers and gyroscopes are derived. To achieve this goal, at first, the misalignment value is obtained by using the equations of small rotation angles.

Rotation of Small Angles

Small angle equations are used for two reasons. First, the misalignment in this research is small, and secondly, the main focus in this research is on obtaining biases, otherwise, there are equations for larger misalignment that are given in. When the rotation angles are small, the following relationship exists between the two frames [18]:

$$\mathbf{\Phi}^{\hat{\mathrm{N}}\mathrm{N}} = \mathbf{I} + \varepsilon\, \mathbf{\Phi} \tag{1}$$

Where $\Phi^{\hat{\mathrm{N}}\mathrm{N}}$ is the rotation tensor of the estimated navigation frame ($\hat{\mathrm{N}}$) with respect to the true navigation frame (N); $\mathbf{I}$ is the identity tensor and $\varepsilon\Phi^{\hat{\mathrm{N}}\mathrm{N}}$ is the skew-symmetric form of the perturbation tensor ($\varepsilon\Phi^{\hat{\mathrm{N}}\mathrm{N}}$), which is modeled as follows:

$$\begin{aligned}
&\left[\mathbf{\Phi}^{\hat{\mathrm{N}}\mathrm{N}}\right]^{N} = [\,\varepsilon\ \varphi\ \ \varepsilon\ \theta\ \ \varepsilon\ \psi]^{N} \rightarrow \\
&\left[\mathbf{\Phi}^{\hat{\mathrm{N}}\mathrm{N}}\right]^{N} = \begin{bmatrix} 0 & -\varepsilon\ \psi & \varepsilon\ \theta \\ \varepsilon\ \psi & 0 & -\varepsilon\ \varphi \\ -\varepsilon\ \theta & \varepsilon\ \varphi & 0 \end{bmatrix}
\end{aligned} \tag{2}$$

In the previous equation, $\varepsilon\varphi$, $\varepsilon\theta$ and $\varepsilon\psi$ represent three small rotation angles. According to reference [18], the relationship $\left[\Phi^{\hat{\mathrm{N}}\mathrm{N}}\right]^{N} = [\mathrm{T}]^{\hat{\mathrm{N}}\mathrm{N}}$ where $[\mathrm{T}]^{\hat{\mathrm{N}}\mathrm{N}}$ defines the transformation matrix that converts coordinates from the N frame to the $\hat{\mathrm{N}}$ frame. By applying this transformation, Equation (1) can be reformulated in the navigation frame as follows:

$$\begin{aligned}
&[\varepsilon\mathbf{\Phi}^{\hat{\mathrm{N}}\mathrm{N}}]^{\mathrm{N}} = [\mathbf{\Phi}^{\hat{\mathrm{N}}\mathrm{N}}]^{\mathrm{N}} - [\mathbf{I}]^{\mathrm{N}} = \\
&[\overline{\mathrm{T}}]^{\hat{\mathrm{N}}\mathrm{N}} - [\mathbf{I}]^{\mathrm{N}} = [\mathrm{T}]^{\mathrm{N}\hat{\mathrm{N}}} - [\mathbf{I}]^{\mathrm{N}} = \\
&[\mathrm{T}]^{\mathrm{NB}}[\mathrm{T}]^{\mathrm{B}\hat{\mathrm{N}}} - [\mathbf{I}]^{\mathrm{N}}
\end{aligned} \tag{3}$$

Where $[\mathrm{T}]^{\mathrm{BN}}$ is a matrix function that transforms navigation into a body frame and $[\mathrm{T}]^{\mathrm{BN}} = f(\psi,\theta,\varphi)$ and $[\mathrm{T}]^{\mathrm{B}\hat{\mathrm{N}}} = f(\hat{\psi},\hat{\theta},\hat{\varphi})$; where φ,θ,ψ are true and $\hat{\psi},\hat{\theta},\hat{\varphi}$ are estimated Euler angles.

In reference [19], the relationship between the master and slave frames is established, and the resulting expression is presented below.

$$\begin{cases}
\varepsilon\varphi = (\hat{\theta}-\bar{\theta})\sin\bar{\psi} - (\hat{\varphi}-\bar{\varphi})\cos\bar{\psi}\cos\bar{\theta} \\
\quad -(\hat{\psi}-\bar{\psi})(\hat{\theta}-\bar{\theta})\cos\bar{\psi} \\
\quad -(\hat{\varphi}-\bar{\varphi})(\hat{\psi}-\bar{\psi})\cos\bar{\theta}\sin\bar{\psi} \\
\\
\varepsilon\theta = -(\hat{\theta}-\bar{\theta})\cos\bar{\psi} \\
\quad -(\hat{\varphi}-\bar{\varphi})\cos\bar{\theta}\sin\bar{\psi} \\
\quad -(\hat{\varphi}-\bar{\varphi})(\hat{\theta}-\bar{\theta})\sin\bar{\psi}\sin\bar{\theta} \\
\\
\varepsilon\psi = (\hat{\varphi}-\bar{\varphi})\sin\bar{\theta} - (\hat{\psi}-\bar{\psi}) \\
\quad -(\hat{\varphi}-\bar{\varphi})(\hat{\theta}-\bar{\theta})\cos^2\bar{\psi}\cos\bar{\theta} \\
\quad -(\hat{\varphi}-\bar{\varphi})(\hat{\psi}-\bar{\psi})(\hat{\theta}-\bar{\theta})\cos\bar{\psi}\cos\bar{\theta}\sin\bar{\psi}
\end{cases} \tag{4}$$

The above equation demonstrates the relationship between the small rotation angles and the Euler angles. Expansion of Eq. (4) is also as follows:

$$\begin{cases}
\varepsilon\varphi = \hat{\theta}\sin\bar{\psi} - \bar{\theta}\sin\bar{\psi} - \hat{\varphi}\cos\bar{\psi}\cos\bar{\theta} \\
\quad +\bar{\varphi}\cos\bar{\psi}\cos\bar{\theta} + \hat{\psi}\bar{\theta}\cos\bar{\psi} \\
\quad -\hat{\psi}\hat{\theta}\cos\bar{\psi} + \bar{\psi}\hat{\theta}\cos\bar{\psi} - \bar{\psi}\bar{\theta}\cos\bar{\psi} \\
\quad +\hat{\varphi}\bar{\psi}\cos\bar{\theta}\sin\bar{\psi} - \hat{\varphi}\hat{\psi}\cos\bar{\theta}\sin\bar{\psi} \\
\quad +\bar{\varphi}\hat{\psi}\cos\bar{\theta}\sin\bar{\psi} - \bar{\varphi}\bar{\psi}\cos\bar{\theta}\sin\bar{\psi} \\
\\
\varepsilon\theta = -\hat{\theta}\cos\bar{\psi} + \bar{\theta}\cos\bar{\psi} - \hat{\varphi}\cos\bar{\theta}\sin\bar{\psi} \\
\quad +\bar{\varphi}\cos\bar{\theta}\sin\bar{\psi} + \hat{\varphi}\bar{\theta}\sin\bar{\psi}\sin\bar{\theta} \\
\quad -\hat{\varphi}\hat{\theta}\sin\bar{\psi}\sin\bar{\theta} + \bar{\varphi}\hat{\theta}\sin\bar{\psi}\sin\bar{\theta} \\
\quad -\bar{\varphi}\bar{\theta}\sin\bar{\psi}\sin\bar{\theta} \\
\\
\varepsilon\psi = \hat{\varphi}\sin\bar{\theta} - \bar{\varphi}\sin\bar{\theta} - \hat{\psi} + \bar{\psi} \\
\quad +\hat{\varphi}\bar{\theta}\cos^2\bar{\psi}\cos\bar{\theta} - \hat{\varphi}\hat{\theta}\cos^2\bar{\psi}\cos\bar{\theta} \\
\quad +\bar{\varphi}\hat{\theta}\cos^2\bar{\psi}\cos\bar{\theta} - \bar{\varphi}\bar{\theta}\cos^2\bar{\psi}\cos\bar{\theta} \\
\quad +\hat{\varphi}\hat{\psi}\bar{\theta}\cos\bar{\psi}\cos\bar{\theta}\sin\bar{\psi} \\
\quad -\hat{\varphi}\hat{\psi}\hat{\theta}\cos\bar{\psi}\cos\bar{\theta}\sin\bar{\psi} \\
\quad +\hat{\varphi}\bar{\psi}\hat{\theta}\cos\bar{\psi}\cos\bar{\theta}\sin\bar{\psi} \\
\quad +\bar{\varphi}\hat{\psi}\hat{\theta}\cos\bar{\psi}\cos\bar{\theta}\sin\bar{\psi} \\
\quad -\hat{\varphi}\bar{\psi}\bar{\theta}\cos\bar{\psi}\cos\bar{\theta}\sin\bar{\psi} \\
\quad -\bar{\varphi}\hat{\psi}\bar{\theta}\cos\bar{\psi}\cos\bar{\theta}\sin\bar{\psi} \\
\quad -\bar{\varphi}\bar{\psi}\hat{\theta}\cos\bar{\psi}\cos\bar{\theta}\sin\bar{\psi} \\
\quad +\bar{\varphi}\bar{\psi}\bar{\theta}\cos\bar{\psi}\cos\bar{\theta}\sin\bar{\psi}
\end{cases} \tag{5}$$

According to Eq [5], the difference between the master and slave frames has been calculated, which is referred to as

misalignment.

Bias Estimation equation

To estimate the bias of the accelerometer and gyroscope, the set of navigation error equations for speed and attitude should be considered first. These equations are given in [6-7] as follows:

$$\begin{cases}
\varepsilon\dot{v}_n = T_{11}^{NB}\delta f_x + T_{12}^{NB}\delta f_y + T_{13}^{NB}\delta f_z \\
\quad + f_e\varepsilon\psi - f_d\varepsilon\theta - (\frac{v_e{}^2\sec^2\lambda}{R_e} + 2\omega_n v_e)\varepsilon\lambda \\
\quad + \frac{(v_e{}^2\tan\lambda - v_n v_d)}{R_e{}^2}\varepsilon h + \frac{v_d}{R_e}\varepsilon v_n \\
\quad + (2\omega_d - \frac{2v_e\tan\lambda}{R_e})\varepsilon v_e + \frac{v_n}{R_e}\varepsilon v_d \\
\varepsilon\dot{v}_e = T_{21}^{NB}\delta f_x + T_{22}^{NB}\delta f_y + T_{23}^{NB}\delta f_z - f_n\varepsilon\psi \\
\quad + f_d\varepsilon\varphi + (\frac{v_e v_n\sec^2\lambda}{R_e} + 2\omega_n v_n + 2\omega_d v_d)\varepsilon\lambda \\
\quad - \frac{(v_e v_n\tan\lambda + v_e v_d)}{R_e{}^2}\varepsilon h + (\frac{v_e}{R_e} + 2\omega_n)\varepsilon v_d \\
\quad + (\frac{v_e\tan\lambda}{R_e} - 2\omega_d)\varepsilon v_n + \frac{(v_n\tan\lambda + v_d)}{R_e}\varepsilon v_e \\
\varepsilon\dot{v}_d = T_{31}^{NB}\delta f_x + T_{32}^{NB}\delta f_y + T_{33}^{NB}\delta f_z \\
\quad + f_n\varepsilon\theta - f_e\varepsilon\varphi - 2\omega_d v_e\varepsilon\lambda + \frac{(v_e{}^2 + v_n{}^2)}{R_e{}^2}\varepsilon h \\
\quad + \delta g - \frac{2v_n}{R_e}\varepsilon v_n - (\frac{2v_e}{R_e} + 2\omega_n)\varepsilon v_e
\end{cases} \tag{6}$$

$$\begin{cases}
\varepsilon\dot{\varphi} = \omega_d\varepsilon\lambda - \frac{v_e}{R_e{}^2}\varepsilon h + \frac{1}{R_e}\varepsilon v_e \\
\quad + (\omega_d - \frac{v_e\tan\lambda}{R_e})\varepsilon\theta + \frac{v_n}{R_e}\varepsilon\psi \\
\quad - T_{11}^{NB}\delta\omega_x - T_{12}^{NB}\delta\omega_y - T_{13}^{NB}\delta\omega_z \\
\varepsilon\dot{\theta} = \frac{v_n}{R_e{}^2}\varepsilon h - \frac{1}{R_e}\varepsilon v_n \\
\quad + (\frac{v_e\tan\lambda}{R_e} - \omega_d)\varepsilon\varphi + (\omega_n + \frac{v_e}{R_e})\varepsilon\psi \\
\quad - T_{21}^{NB}\delta\omega_x - T_{22}^{NB}\delta\omega_y - T_{23}^{NB}\delta\omega_z \\
\varepsilon\dot{\psi} = -(\omega_n + \frac{v_e\sec^2\lambda}{R_e})\varepsilon\lambda + \frac{v_e\tan\lambda}{R_e{}^2}\varepsilon h \\
\quad - \frac{\tan\lambda}{R_e}\varepsilon v_e - \frac{v_n}{R_e}\varepsilon\varphi - (\omega_n + \frac{v_e}{R_e})\varepsilon\theta \\
\quad - T_{31}^{NB}\delta\omega_x - T_{32}^{NB}\delta\omega_y - T_{33}^{NB}\delta\omega_z
\end{cases} \tag{7}$$

In this context, λ & ℓ represents latitude and longitude, while vn, ve, and vd refer to the terrestrial velocities in the north, east, and downward directions, respectively. Re denotes the Earth's radius, and ε serves as the perturbation operator. The attitude errors between the actual and computed navigation frames are indicated by εφ, εθ, and εψ. Furthermore, $\grave{u}^{EI}$ signifies the Earth's angular velocity, whereas ωn, ωd, fn, fe, and fd are defined as follows:

$$[\boldsymbol{\omega}^{EI}]^N = \begin{bmatrix} \omega^{EI}\cos\lambda \\ 0 \\ -\omega^{EI}\sin\lambda \end{bmatrix} = \begin{bmatrix} \omega_n \\ 0 \\ \omega_d \end{bmatrix} \tag{8}$$

$$[\mathbf{a}_B^I]^N = \begin{bmatrix} f_n \\ f_e \\ f_d \end{bmatrix} = [T]^{NB}\begin{bmatrix} f_x \\ f_y \\ f_z \end{bmatrix} \tag{9}$$

Eq [10-11] can be derived by using Eq [6-7], where the bias values of accelerometers and gyroscopes are obtained. It should be noted that the stationary mode assumption is not used in these equations, and they also can be used for the in-motion transfer alignment.

3- Simulation

The simulation is presented in this section. The main focus of the simulation is on estimating the bias of accelerometers and gyroscopes, using experimental data from both. The simulation is divided into two parts: data generation and bias compensation.

Data generation requires two sets of data: accurate and less accurate. Accurate data is obtained from experimental data, while less accurate data involves adding bias and white noise to the experimental data.

The bias considered for the accelerometer in the X, Y, and Z axes is 0.001, 0.002, and 0.003 m/s^2, respectively, while for the gyroscope in the X, Y, and Z axes the bias value is 1e^{-8}, 5e^{-8}, and 8e^{-8} rad/s respectively. The noise level for the sensors should not exceed the bias and should be at least one order of magnitude lower than the bias of the sensors. Data from accelerometers and gyroscopes are displayed in Figures 1 and 2. Based on the accelerometer data presented in Figure 2, it is evident that the vehicle is not stationary and is experiencing a constant acceleration in the X-axis, leading to an increase in

$$\begin{bmatrix}\delta f_x\\ \delta f_y\\ \delta f_z\end{bmatrix}=[\mathrm{T^{NB}}]^{-1}\begin{bmatrix}\varepsilon\dot{v}_n\\ \varepsilon\dot{v}_e\\ \varepsilon\dot{v}_d\end{bmatrix}-[\mathrm{T^{NB}}]^{-1}\begin{bmatrix} f_e\varepsilon\psi-f_d\varepsilon\theta-(\frac{v_e^{\,2}\sec^2\lambda}{R_e}+2\omega_n v_e)\varepsilon\lambda+\frac{(v_e^{\,2}\tan\lambda-v_n v_d)}{R_e^{\,2}}\varepsilon h\\ +\frac{v_d}{R_e}\varepsilon v_n+(2\omega_d-\frac{2v_e\tan\lambda}{R_e})\varepsilon v_e+\frac{v_n}{R_e}\varepsilon v_d\\ -f_n\varepsilon\psi+f_d\varepsilon\varphi+(\frac{v_e v_n\sec^2\lambda}{R_e}+2\omega_n v_n+2\omega_d v_d)\varepsilon\lambda\\ -\frac{(v_e v_n\tan\lambda+v_e v_d)}{R_e^{\,2}}\varepsilon h+(\frac{v_e}{R_e}+2\omega_n)\varepsilon v_d\\ f_n\varepsilon\theta-f_e\varepsilon\varphi-2\omega_d v_e\varepsilon\lambda+\frac{(v_e^{\,2}+v_n^{\,2})}{R_e^{\,2}}\varepsilon h\\ +\delta g-\frac{2v_n}{R_e}\varepsilon v_n-(\frac{2v_e}{R_e}+2\omega_n)\varepsilon v_e\end{bmatrix} \tag{10}$$

$$\begin{bmatrix}\delta\omega_x\\ \delta\omega_y\\ \delta\omega_z\end{bmatrix}=-[\mathrm{T^{NB}}]^{-1}\begin{bmatrix}\varepsilon\dot{\varphi}\\ \varepsilon\dot{\theta}\\ \varepsilon\dot{\psi}\end{bmatrix}+[\mathrm{T^{NB}}]^{-1}\begin{bmatrix}\omega_d\varepsilon\lambda-\frac{v_e}{R_e^{\,2}}\varepsilon h+\frac{1}{R_e}\varepsilon v_e+(\omega_d-\frac{v_e\tan\lambda}{R_e})\varepsilon\theta+\frac{v_n}{R_e}\varepsilon\psi\\ \frac{v_n}{R_e^{\,2}}\varepsilon h-\frac{1}{R_e}\varepsilon v_n+(\frac{v_e\tan\lambda}{R_e}-\omega_d)\varepsilon\varphi+(\omega_n+\frac{v_e}{R_e})\varepsilon\psi\\ -(\omega_n+\frac{v_e\sec^2\lambda}{R_e})\varepsilon\lambda+\frac{v_e\tan\lambda}{R_e^{\,2}}\varepsilon h-\frac{\tan\lambda}{R_e}\varepsilon v_e-\frac{v_n}{R_e}\varepsilon\varphi-(\omega_n+\frac{v_e}{R_e})\varepsilon\theta\end{bmatrix} \tag{11}$$

speed in the X-axis direction.

As mentioned before, this simulator uses experimental data, and the following initial conditions are utilized: The roll and pitch angle initial values are set to zero, with an initial speed of 50 m/s that gradually increases. The experiment has been investigated at various heading angles. Based on this maneuver, it can be concluded that the device can estimate the bias of the accelerometer and gyroscope in acceleration mode, at different headings. The results obtained regarding the estimation of sensor biases and estimation speed will be presented in the next section.

4- Experiment

One of the results obtained from the proposed algorithm is the misalignment angles. This method has a suitable speed and quickly estimates the misalignment values. The misalignment and rate of misalignment are shown in Figures 3 and 4. The bias values of accelerometers and gyroscopes are calculated in the next step.

The bias values of the accelerometer and gyroscope are shown in Figures 5 and 6. According to the figures, this algorithm was able to accurately estimate the bias of both the accelerometer and gyroscope. While this algorithm operates at a high speed, one of its drawbacks is the presence of noise in the data. To handle this issue, a low-pass filter can be utilized.

A low-pass filter is utilized to eliminate the noise in this algorithm. Although this method may slow down the algorithm and require approximately three seconds for estimation, this time frame is ideal for accurate estimation and justifies the use of the low-pass filter to remove system noises. Filter transform function equal to $\frac{S}{S+1}$ this filter

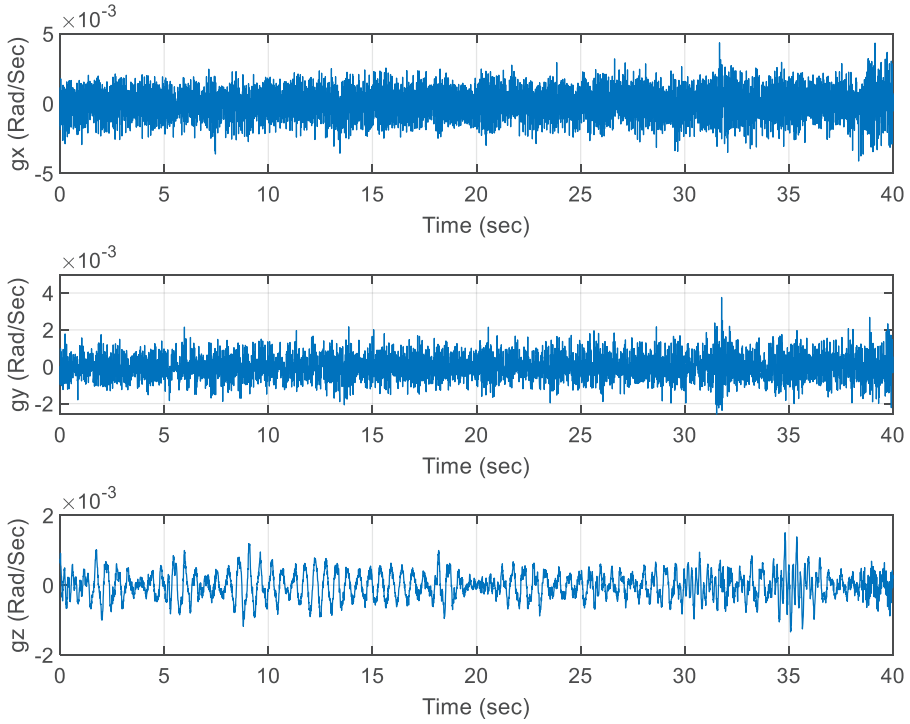

Fig. 1. Angular velocity of sensors

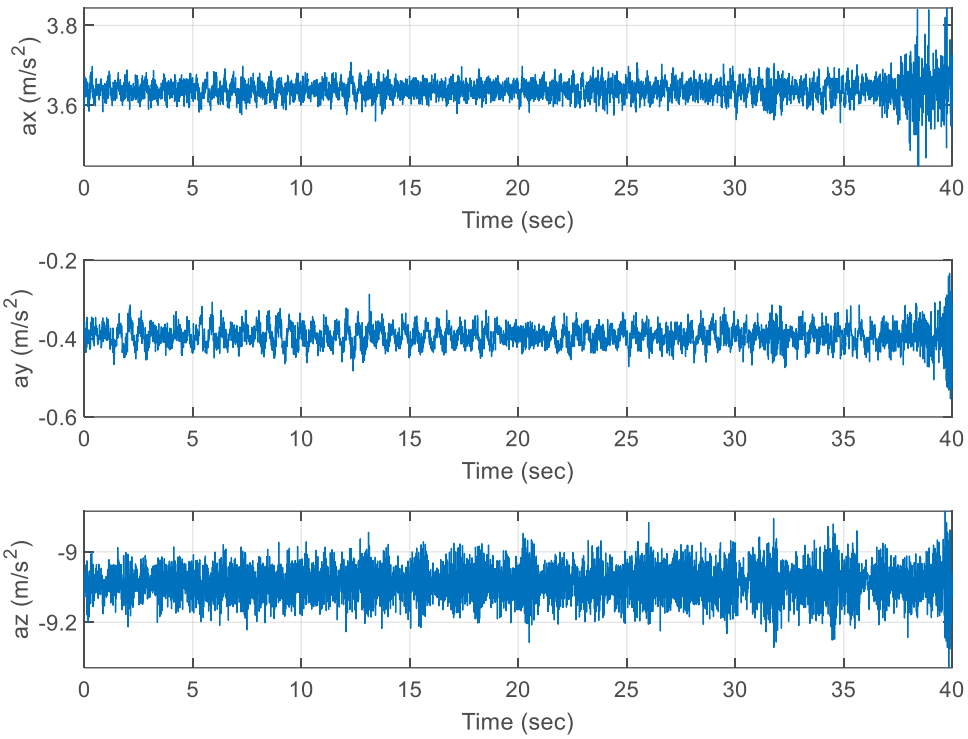

Fig. 2. Acceleration data with bias & noise

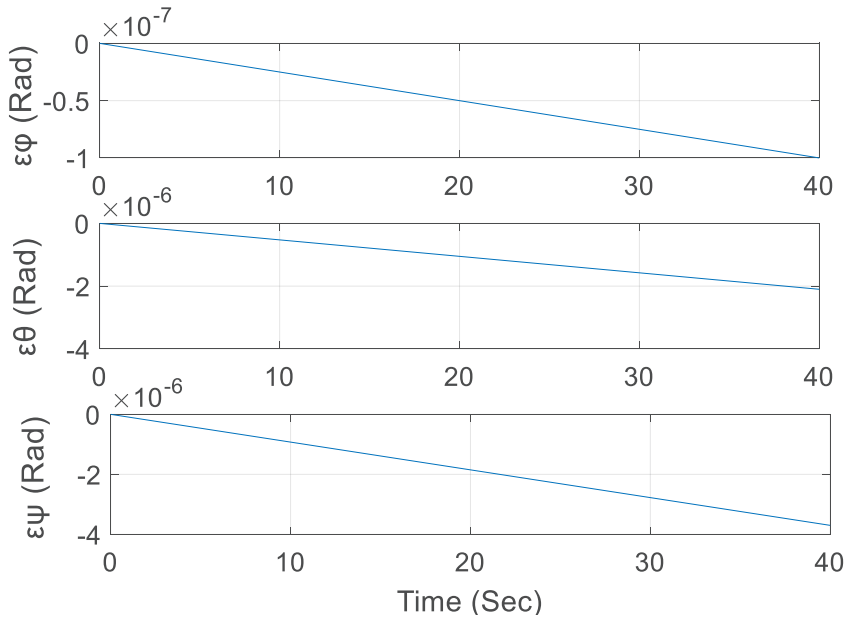

Fig. 3. Misalignment between the navigation and sensor frames

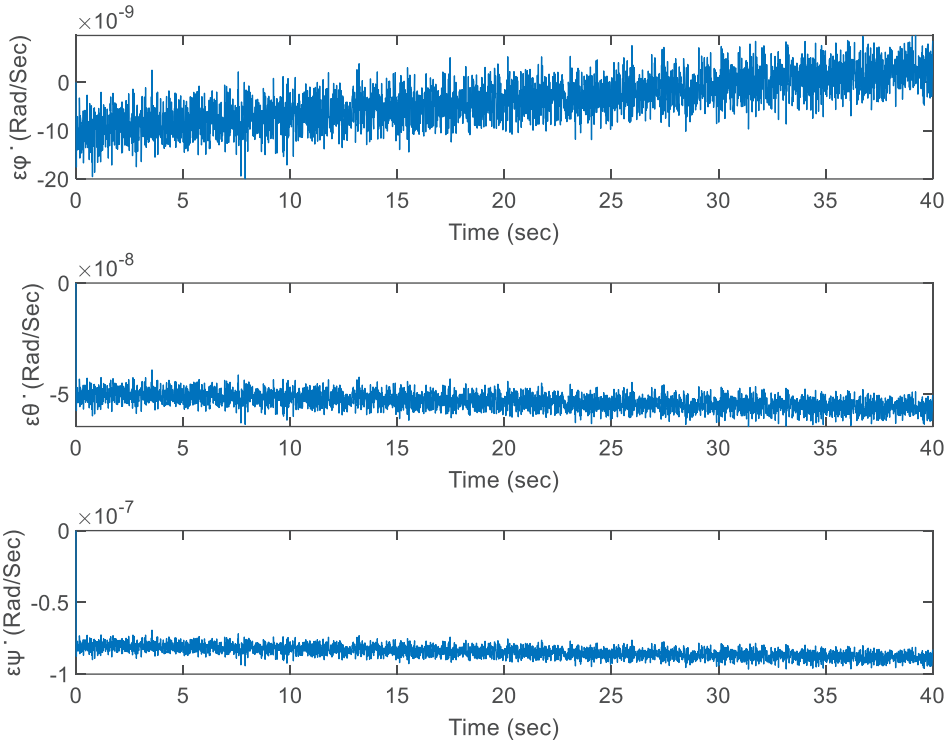

Fig. 4. Rate of misalignment between navigation and sensor frames

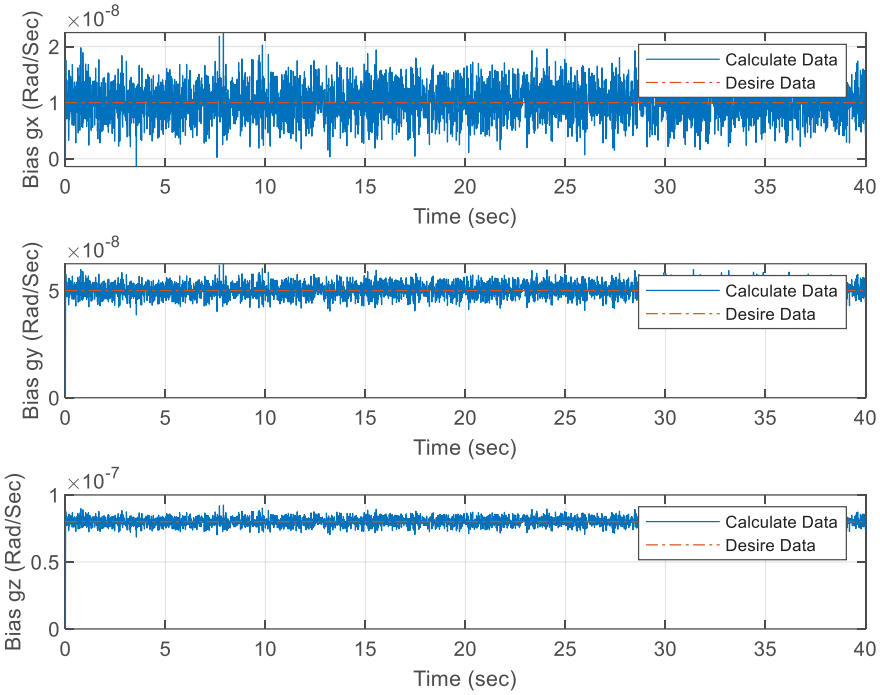

Fig. 5. Gyro Bias without using low pass filter

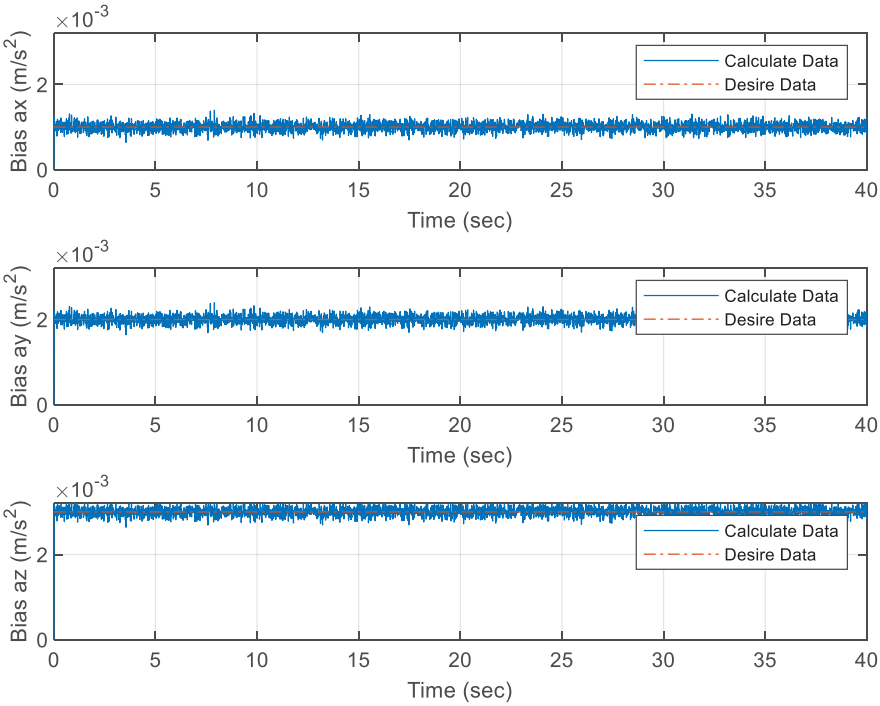

Fig. 6. Acceleration bias without using low pass filter

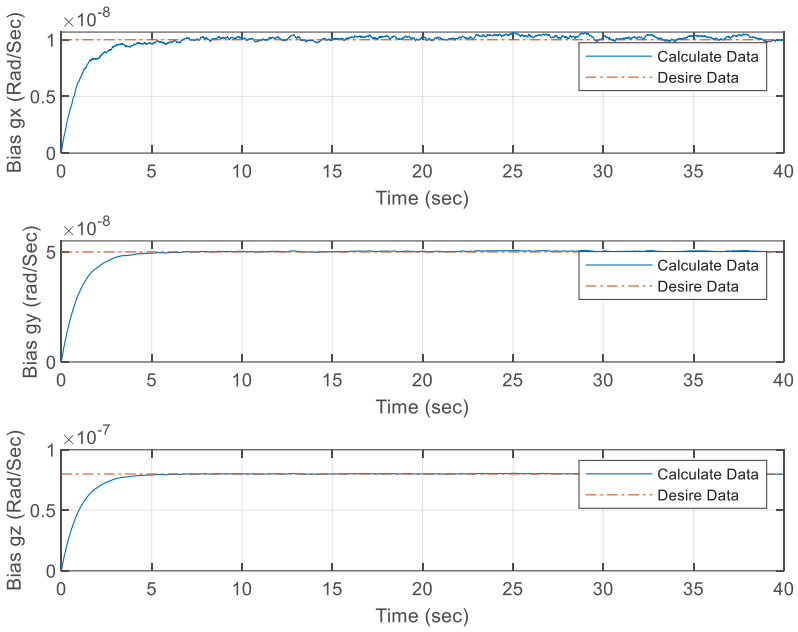

Fig. 7. Gyro Bias with low pass filter

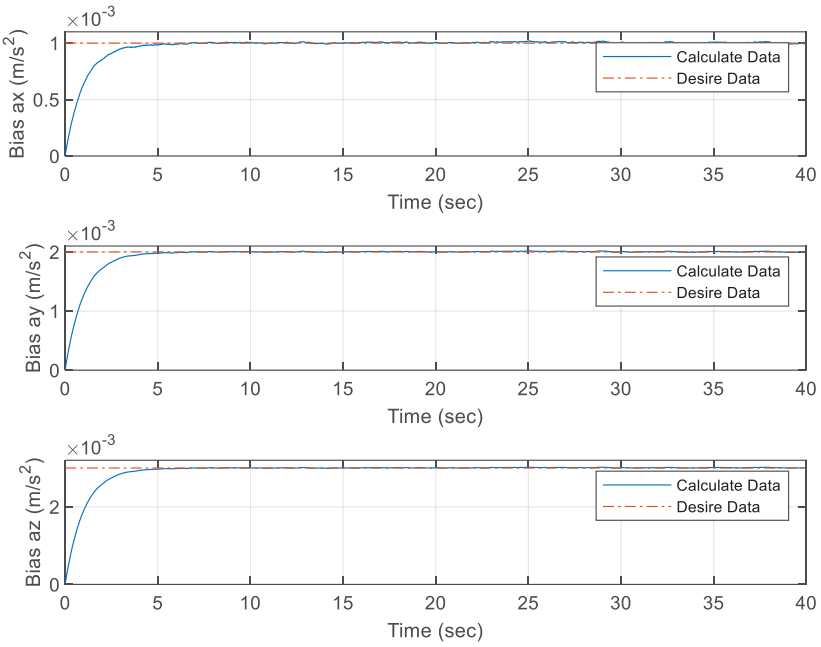

Fig. 8. Acceleration bias with low pass filter

works by trial and error because it removes noise well. The bias estimated without noise is depicted in Figures 7 and 8.

5- Conclusion

In this article, the bias values of the accelerometer and gyroscope are estimated using navigation error equations and real measured values from two sensors, one accurate and the other less accurate. Initially, misalignment values are calculated through a small angle of rotation by comparing actual and measured values, taking into account misalignment between the master and slave frame.

In the navigation error equation, three accelerometer biases and three gyroscope biases are determined by solving six navigation error equations numerically. This bias calculation method is efficient and can be considered as one of the important achievements of this study.

The proposed algorithm also calculates the misalignment angles between the master and slave frames. It estimates the bias in the accelerometer and gyroscope based on the misalignment values. Finally, accelerometer and gyroscope noise is eliminated using a low-pass filter. The approximate time required to calculate the bias estimation in this algorithm is about three seconds, which can be classified as a fast algorithm.

References

[1] R. M. Rogers, Applied Mathematics in Integrated Navigation Systems, Gainesville, Florida: American Institute of Aeronautics and Astronautics (AIAA), 2007.

[2] W. Li, W. Wu, J. Wang, and L. Lu, "A Fast SINS Initial Alignment Scheme for Underwater Vehicle Applications," The Journal Of Navigation, vol. 66, p. 181–198, 2012.

[3] A. Ramanandan, A. Chen and J. Farrell, "Inertial navigation aiding by stationary updates," Intelligent Transportation Systems, IEEE Transactions on 13.1, pp. 235-248, 2012.

[4] F. O. Silva, W. C. L. Filho, and E. M. Hemerly, "Design of a Stationary Self-Alignment Algorithm for Strapdown Inertial," in International Federation of Automatic Control, 2015.

[5] Cheng Ma, Shiyin Zhou, "In-motion fine alignment algorithm for AUV based on improved extended state observer and Kalman filter", DOI:10.1088/1361-6501/ad7876, September 2024

[6] Jun Li, Shifeng Zhang, Huabo Yang, Zhenyu Jiang, Xibin Bai, "Fast Alignment and Calibration of Rotational Inertial System Based on Bilinear Embedding", Page(s): 10700 – 10713, IEEE Sensors Journal (Volume: 24, Issue: 7, 01 April 2024)

[7] L. Zhu and X. Cheng, "An Improved Initial Alignment Method for Rocket Navigation Systems," The Journal Of Navigation, vol. 66, p. 737–749, 2013.

[8] F. O. Silva, E. M. Hemerly, and W. C. L. Filho, "Error Analysis of Analytical Coarse Alignment Formulations for Stationary SINS," IEEE Transactions On Aerospace And Electronic Systems, Vols. 52, No.4, 2016.

[9] F. O. E. Silva, E. M. Hemerly, W. d. C. L. Filho, and R. A. J. Chagas, "An Improved Stationary Fine Self-Alignment Approach for SINS Using Measurement Augmentation," in Anais do XX Congresso Brasileiro de Automática, Belo Horizonte, 2014.

[10] H. Li, Q. Pan, X. Wang, X. Jiang and L. Deng, "Kalman Filter Design for Initial Precision Alignment of a Strapdown Inertial Navigation System on a Rocking Base," The Journal of Navigation, vol. 68, pp. 184-195, 2014.

[11] J. Li, J. Xu, L. Chang, and F. Zha, "An Improved Optimal Method for Initial Alignment," The Journal Of Navigation, vol. 67, pp. 727-736, 2014.

[12] C. G. Park and J. G. Lee, "An overlapping decomposed filter for INS initial alignment," Journal of the Korean Society for Aeronautical and Space Sciences 19.3, pp. 65-76, 1991.

[13] W. Gao, Y. Zhang, and J. Wang, "Research on Initial Alignment and Self-Calibration of Rotary Strapdown Inertial Navigation Systems," Sensors, vol. 15, pp. 3154-3171, 2015.

[14] Jianhua Cheng, Jing Cai, Zhenmin Wang, And Jiaxin Liu, "A Novel Polar Rapid Transfer Alignment For Shipborne Sins Under Arbitrary Misalignments", Volume 8, 2020

[15] J Yang, X Wang, B Wang, X Hu," A high-accuracy system model and accuracy evaluation method for transfer alignment", Measurement Science and Technology, 2024

[16] J Yang, X Wang, X Ji, X Hu, G Nie," A new high-accuracy transfer alignment method for distributed INS on moving base", Measurement Volume 227, March 2024

[17] Laetitia Tosoni, Minh Tu Pham, Paolo Massioni, Elliot Broussard. Rapid transfer alignment for large and time-varying attitude misalignment angles. IEEE Control Systems Letters, 2023, pp.1-6. ff10.1109.

[18] P. H. Zipfel, Modeling and simulation of aerospace vehicle dynamics, AIAA, 2007

[19] M. A. Amiri Atashgah, Hamed Mohammadkarimi, Mehrdad Ebrahimi," A fast strapdown gyrocompassing algorithm based on INS differential errors", Scientific Reports volume 13, Article number: 15297 (2023)

HOW TO CITE THIS ARTICLE

R. Soltani Nejad, H. Mohammad Karimi, A. Naghash, Online Error Estimation of Inertial Measurement Unit in Transfer Alignment Problem, AUT J. Model. Simul., 56(2) (2024) 199-208.

DOI: 10.22060/miscj.2025.23614.5391